Machine Learning Methods and Docking for Predicting Human Pregnane X Receptor Activation

Akash Khandelwal,[†] Matthew D. Krasowski,[‡] Erica J. Reschly,[‡] Michael W. Sinz,[§] Peter W. Swaan,[†] and Sean Ekins*[,†,||,⊥]

Department of Pharmaceutical Sciences, University of Maryland, 20 Penn Street, Baltimore, Maryland 21201, Department of Pathology, University of Pittsburgh, Pittsburgh, Pennsylvania 15261, Bristol-Myers Squibb Company, Research Parkway, Wallingford, Connecticut 06492, Department of Pharmacology, University of Medicine and Dentistry of New Jersey, Robert Wood Johnson Medical School, 675 Hoes Lane, Piscataway, New Jersey 08854, and Collaborations in Chemistry, 601 Runnymede Avenue, Jenkintown, Pennsylvania 19046

Received March 12, 2008

The pregnane X receptor (PXR) regulates the expression of genes involved in xenobiotic metabolism and transport. In vitro methods to screen for PXR agonists are used widely. In the current study, computational models for human PXR activators and PXR nonactivators were developed using recursive partitioning (RP), random forest (RF), and support vector machine (SVM) algorithms with VolSurf descriptors. Following 10-fold randomization, the models correctly predicted 82.6−98.9% of activators and 62.0−88.6% of nonactivators. The models were validated using separate test sets. The overall (n = 15) test set prediction accuracy for PXR activators with RP, RF, and SVM PXR models is 80−93.3%, representing an improvement over models previously reported. All models were tested with a second test set (n = 145), and the prediction accuracy ranged from 63 to 67% overall. These test set molecules were found to cover the same area in a principal component analysis plot as the training set, suggesting that the predictions were within the applicability domain. The FlexX docking method combined with logistic regression performed poorly in classifying this PXR test set as compared with RP, RF, and SVM but may be useful for qualitative interpretion of interactions within the LBD. From this analysis, VolSurf descriptors and machine learning methods had good classification accuracy and made reliable predictions within the model applicability domain. These methods could be used for high throughput virtual screening to assess for PXR activation, prior to in vitro testing to predict potential drug−drug interactions.

Introduction

The human pregnane X receptor, PXR[1] (NR1I2; also known as SXR or PAR) is a transcriptional regulator of a large number of genes involved in xenobiotic metabolism and excretion. The genes regulated by PXR include cytochrome P450 (CYP) 3A4 (*1–3*), CYP2B6 (*4*), aldehyde dehydrogenases, glutathione-*S*-transferase, sulfotransferases, organic anion transporter peptide 2, and multidrug resistance proteins 1 and 2 (*5, 6*) as well as others. Human PXR activators include a wide range of prescription and herbal drugs such as paclitaxel, troglitazone, rifampicin, ritonavir, clotrimazole, and St. John's Wort, which can be involved in clinically relevant drug−drug interactions (*7*). In addition to xenobiotics, PXR is also activated by pregnanes, androstanes, bile acids, hormones, dietary vitamins, and a wide array of endogenous molecules recently reviewed (*8*).

The PXR ligand-binding domain (LBD) consists of 12 α-helices that fold to form a hydrophobic pocket and a short region of β-strands. The pocket is lined with 28 amino acid residues, 10 hydrophobic, four polar, and four charged (*9–13*). The potential for molecules to bind in numerous locations in the LBD complicates the reliable prediction of PXR activators (A) or nonactivators (N) using structure-based drug design methods alone. Computational models ranging from ligand-based pharmacophores (*14–17*), quantitative structure−activity relationships (QSAR) (*18–20*), and machine learning methods (*20*) to homology modeling with molecular dynamics (*21*) (for identifying protein−corepressor interactions), represent predominantly reports to predict PXR ligand binding (*8*) to differing degrees. These previously described computational methods focused on diverse structural types for agonists and in one case used structural analogues (*8*), which may have assessed specific binding locations within the LBD, such as that for steroidal compounds. A likely consensus has emerged across the different QSAR modeling methods that PXR agonists are required to fit to multiple hydrophobic features and at least one hydrogen bond acceptor (and in some cases an additional hydrogen bond donor feature) (*8*). A further qualitative observation from these previous studies is the dependence of the resulting agonist QSAR or pharmacophore models on the molecules used in the training set and potential for overlap of multiple models derived from different molecules (*8*). It should also be noted that rarely do the published QSAR models utilize a large external test set to validate the predictive nature or assess the applicability domain (*22–24*) of the training and test sets; that is, how structurally similar do the molecules in the training and test set have to be for accurate predictions? This is especially important to build confidence in the use of these methods with such

* To whom correspondence should be addressed. Tel: 269-930-0974. Fax: 215-481-0159. E-mail: ekinssean@yahoo.com.
[†] University of Maryland.
[‡] University of Pittsburgh.
[§] Bristol-Myers Squibb Company.
[||] Robert Wood Johnson Medical School.
[⊥] Collaborations in Chemistry.

[1] Abbreviations: ADME/Tox, absorption, distribution, metabolism excretion/toxicology; LBD, ligand-binding domain; PCA, principal component analysis; PXR, pregnane X receptor; PDB, Protein Data Bank; QSAR, quantitative structure−activity relationship; RF, random forest; RP, recursive partitioning; SVM, support vector machine.

10.1021/tx800102e CCC: $40.75

structurally promiscuous proteins as PXR. One of the limitations of using published data for PXR is that only a small fraction of the data available reports quantitative EC_{50} data (for example, much of the work is published as greater or less than a cutoff value, e.g., 100 μM). Therefore, there are currently no widely available large, diverse continuous data sets to enable quantitative QSAR modeling for human PXR. Two PXR machine learning studies have been published recently with relatively large training sets (≥99 molecules) using recursive partitioning (*19*), support vector machine (SVM), *K*-nearest neighbors (*k*-NN), and probabilistic neural network (PNN) (*20*). In the latter case, binary classification data for 98 human PXR activators and 79 nonactivators were used (*20*) to predict between 80.8 and 85.0% of human PXR activators and 67.7 and 73.6% of human PXR nonactivators (in the training set); the test set prediction accuracies in this same study ranged from 53.3 to 66.7% for 15 known human PXR activators across the three machine learning methods, with SVM performing the best (*20*).

A structure-based alternative to understanding small molecule−protein interactions is to dock molecules into proteins. These methods have resulted in the discovery of novel inhibitors for many targets (*25–28*) and have been applied to proteins such as drug-metabolizing enzymes, which are also relatively promiscuous in their ligand binding (*27–29*). Docking and scoring ligands in target protein-binding sites are challenging processes (*30–32*), and the performance of different implementations of scoring functions has been found to be target-dependent (*33*). The use of consensus scoring has also been recommended to improve the "hit" enrichment (*34*). Docking of a small number of molecules into the PXR structure, 1NRL has been used previously to design molecules that are weaker agonists (*35*), and an automated docking method (GOLD (*36*), which maintains the protein as rigid) was used to flexibly dock azole PXR antagonists onto the outer surface at the AF-2 site (*8*). We are not aware of any studies using docking as a screening tool to predict the potential for PXR activation on a larger scale with diverse druglike libraries of molecules, and this may be due to the challenge of the protein promiscuity.

In the current study, we have compared recursive partitioning (RP), random forest (RF), and SVM machine learning methods for building human PXR models derived with VolSurf three-dimensional (3D) descriptors [which have been widely applied for absorption, distribution, metabolism excretion/toxicology (ADME/Tox), and drug discovery target modeling (*37–39*)]. In addition, for comparison, we have used FlexX docking (*40, 41*) of molecules into the crystal structures of human PXR combined with logistic regression. The predictive ability of the classification models and docking models was evaluated using a novel large external test set containing 145 human PXR activators and nonactivators (using data for molecules generated in this study and published in the literature) (*42–44*). Our aim was to identify the most appropriate computational approach to predict whether a molecule was likely to be a human PXR agonist (activator) and, in so doing, prioritize molecules for in vitro testing.

Materials and Methods

Reagents and Plasmids. The construction of a HepG2 (human liver) cell line stably expressing human SLC10A1, a transporter that can take up conjugated bile salts, has been reported before in detail (*45*). Human PXR was expressed as a full-length protein, and CYP3A4-PXRE-Luc, which contains promoter elements from CYP3A4 recognized by the PXR DNA-binding domain, was used as the reporter construct. The plasmids for human PXR, human SLC10A1, CYP3A4-PXRE-Luc, and empty vectors pSG5 were generously provided by S. A. Kliewer, J. T. Moore, and L. B. Moore (GlaxoSmithKline, Research Triangle Park, NC).

Reporter Gene Assay with HepG2 Cells. Human PXR activation in the HepG2 human liver cell line was determined by a luciferase-based reporter assay as previously described (*8, 46*).

Data sets and molecular descriptors. A previously published data set was used for model building (training) in which compounds with $EC_{50} < 100$ μM ($n = 98$) were classified as human PXR activators, whereas compounds with $EC_{50} > 100$ μM ($n = 79$) were classified as human PXR nonactivators (*20*). One small test set also published by the same group consisted of 15 human PXR activators (*20*). The molecular structures encoded as SMILES strings (*47*) were downloaded from the Supporting Information tables in the original publication (*20*). We have additionally developed our own novel test set ($n = 145$) consisting of PXR activators ($n = 82$) and PXR nonactivators ($n = 63$) from our exhaustive literature searching (over 5 years) and data generated in this study (see above) that are not in the current training sets (*8, 42, 48*). The SMILES string for each molecule was downloaded from either PubChem (http://pubchem.ncbi.nlm.nih.gov/), ChemSpider (http://www.chemspider.com/), or sketched using the BUILDER module of SYBYL. The SMILES strings for the previously published training and test sets were converted to SYBYL MOL files using an in-house script. The MOL files were then subsequently minimized in SYBYL (Tripos, St. Louis, MO). Energy minimizations were performed using the Tripos force field (*49*) and Gasteiger−Hückel charges with a distance-dependent dielectric constant and conjugate gradient method with a convergence criterion of 0.001 kcal/mol.

Eighty-six VolSurf descriptors (*38*) were calculated from the 3D molecular fields using VolSurf 4.0 implemented in SYBYL. Three different probes including water (OH_2), dry, and amphipathic (BOTH) were used for descriptor calculation. VolSurf descriptors included descriptors for size, shape, hydrophilic and hydrophobic regions, and interaction energy as well as others.

Machine Learning Model Building and Validation. RP calculations were performed using the rpart module of the R package (*50*). Briefly, there are (n) number of compounds, and each compound contains a descriptor (x variables) and a class label (activator or nonactivator). RP is a technique that builds a set of classification rules based on descriptor information. At the base of the tree, all of the n compounds are mixed into a single group. The base is then split into smaller and smaller samples (every subsample is called node) by choosing a descriptor and the corresponding threshold value to divide the sample. If the compound's descriptor value is above the threshold, then it is assigned to one branch, and if it is lower, then it is assigned to the other branch. The ultimate goal is to separate PXR activators from nonactivators. The grown tree can then be used to classify test compounds to activator or nonactivator classes.

The R program was also used for RF calculations (*51*). In the RF method, which is an extension of RP, multiple trees are grown, and predictions are made by averaging the multiple trees. The total number of trees is set to 1000. The other optimizable parameter in the random forest is m_{try}, that is, the number of descriptors (p) randomly sampled as candidates for splitting at each node. The number of descriptors is increased systematically with an increment of 5. The out of bag error (OBB) estimate can be considered as equivalent to a cross-validation study. In OBB, one-third of the compounds is randomly selected as a test set, and a model is developed from the remaining compounds; this is then repeated multiple times. The optimum m_{try} is chosen such that % OBB is a minimum. Thus, a lower % OBB indicates higher accuracy of the model.

The Kernlab package in R was used for generating SVM models using the radial basis kernel function. The grid optimization approach was followed to obtain optimum values of C and γ by varying these parameters from 2^{-5} to 2^{15} and 2^{-15} to 2^{3}, respectively. The optimal C and γ values for the resultant PXR model were 8 and 0.00781, respectively, based on the lowest cross-validation error (*52*).

Table 1. Predictive Performance of RP, RF, SVM, and Docking with Logistic Regression for the Training Set (n = 177, 10-Fold Cross-Validation Study) and Test Set (n = 145)[a]

method	% SE[b]	% SP[c]	% Q[d]	C[e]
		training		
RP	95.92	77.21	87.57	0.754
RF	82.65	62.02	73.45	0.459
SVM	98.98	88.61	94.35	0.888
docking + logistic regression	60.0 (45.92)	40.28 (45.57)	50.34 (45.76)	0.002 (−0.085)
		test set		
RP	64.63	61.9	63.45	0.264
RF	64.63	66.67	65.52	0.310
SVM	68.29	65.08	66.9	0.332
docking + logistic regression	73.42 (70.73)	17.54 (25.4)	50.0 (51.03)	−0.106 (−0.043)

[a] The values in parentheses (docking and logistic regression) include both failed and successfully docked compounds. Key: true positive (TP), true negative (TN), false positive (FP), false negative (FN), sensitivity (SE), specificity (SP), overall prediction accuracy (Q), and Matthew's correlation coefficient (C). [b] SE = TP/(TP + FN). [c] SP = TN/(TN + FP). [d] Q = (TP + TN)/(TP + TN + FP + FN). [e] C = [(TP × TN) − (FN × FP)]/[(TP + FN)(TP + FN)(TN + FN)(TN + FP)]$^{1/2}$.

Docking. The molecules in the training and validation set were docked into four different ligand cocrystallized structures of PXR with hyperforin [Protein Data Bank (PDB) ID: 1M13, resolution 2.00 Å] (*10*), rifampicin (PDB ID: 1SKX, resolution 2.80 Å) (*53*), T0901317 (PDB ID: 2O9I, resolution 2.80 Å) (*54*), and SR12813 (PDB ID: 1NRL, resolution 2.00 Å) (*9*) using FlexX (BioSolveIT, GmbH, Sankt Augustin) (*40, 41*). The FlexX program considered ligand flexibility by an incremental ligand placement technique, while the receptor was considered as rigid. In total, 322 molecules (177 training and 145 testing) were docked into each crystal structure giving rise to 322 × 4 = 1288 molecules. For each ligand (n = 1288), 30 different docked poses were generated (1288 × 30 = 38640 overall poses), and the best pose was selected based on the FlexX score. In all cases, the active site was defined as the amino acid residues within 6 Å of the cocrystallized ligand. The FlexX scores were then used as the independent (x) variable and actual PXR activators (A)/PXR nonactivators (N) as the dependent (y) variable in a logistic regression analysis (eq 1). The PXR activators and PXR nonactivators were assigned scores of 1 and 0, respectively. This logistic regression analysis was performed for molecules docked in all four structures (eq 1).

$$\mathrm{Prob}(Y=\mathrm{A}) = \frac{1}{1+e^{-(\alpha\times\mathrm{FlexX}+\beta)}} \quad \text{or}$$

$$\log \mathrm{odds}(Y=\mathrm{A}) = \alpha\times\mathrm{FlexX}+\beta \quad (1)$$

where, Prob and A represent probability and activator, respectively, and α and β represent adjustable parameters. Two different confusion matrices were built for each crystal structure, that is, one using only successfully docked compounds and the other from both successfully docked and failed compounds. In the latter case, the molecules that failed to dock inside the LBD of PXR were considered as nonactivators.

Data Analysis. The performances of RP, RF, SVM, and docking were evaluated using true positive (TP), true negative (TN), false positive (FP), false negative (FN), sensitivity (SE) [SE = TP/(TP + FN)], specificity (SP) [SP = TN/(TN + FP)], overall prediction accuracy (Q) [Q = (TP + TN)/(TP + TN + FP + FN)], and Matthew's correlation coefficient (C) {C = [(TP × TN) − (FN × FP)]/[(TP + FN)(TP + FP)(TN + FN)(TN + FP)]$^{1/2}$} (Table 1) (*20*). Sensitivity and specificity were used to represent the prediction accuracy of PXR activators and nonactivators, respectively. In the present context, TP is the number of true PXR activators, TN is the number of true PXR nonactivators, FP is the number of falsely classified PXR activators, and FN is the number of falsely classified PXR nonactivators.

Results

The human PXR data for model development (training set n = 177) and a small initial test set (n = 15 activators) were taken from a recent publication (*20*), while the experimental data for the large external test set (n = 145 activators and nonactivators) were collated in the current study and several recent publications (*8, 42, 48*). The predictive performance of RP, RF, and SVM with VolSurf descriptors for predicting PXR activators and PXR nonactivators was initially based on a 10-fold cross-validation metric. A 10-fold cross-validation was chosen to make direct comparisons with previously published models to assess the validity of our selected descriptors and algorithms (*20*). The overall training set prediction accuracies of PXR models were 87.5, 73.4, and 94.3%, respectively (Table 1 and Supplemental Table 1). The C values of the RP, RF, and SVM PXR models were 0.75, 0.46, and 0.89, respectively (Table 1). For comparison, the previous best SVM reported (*20*) had a training set accuracy of 79.6% as compared with 94.3% in this study. The C value ranges between +1 and −1, where a value of +1 indicates perfect prediction, −1 represents an inverse prediction, and 0 indicates that the prediction is equivalent to a completely random prediction. The previous best SVM reported (*20*) had a training set accuracy with a C value of 0.598 as compared with 0.888 in this study. On the basis of the data distribution, the probability of randomly selecting a PXR activator or a PXR nonactivator is 55.4 and 44.6%, respectively. RF would therefore appear to perform poorly as compared with the SVM and RP. The 10-fold cross-validation results would also indicate that in all cases the classification predictions are better than random. All of the models were also validated using external test sets. The first small test set [using 15 known activators from a previous study (*20*)] resulted in a prediction accuracy for RP, RF, and SVM PXR models from 80 to 93.33% (Supplemental Table 1). The previous best SVM reported (*20*) correctly predicted 66.7% of the 15 molecules as compared with 93.33% in this study. Therefore, the overall prediction accuracies for the training and test set machine learning models reported here represent an improvement over the models reported previously using other molecular descriptors (*20*). The large 145 molecule test set (using PXR activators and PXR nonactivators) resulted in overall prediction accuracies for RP, RF, SVM, and the docking PXR logistic regression model of 63.4, 65.5, 66.9, and 51%, respectively (Table 1 and Supplemental Table 2). Interestingly, RF performs better with the external test set than with internal testing for the training set, which would suggest that this model is not overtrained. Consensus scoring has been used previously with QSAR and docking applications (*34, 55–57*) and in some cases can improve predictions over individual methods (*58, 59*). In the current study, a combination of the models indicated that a consensus approach did not improve the overall prediction accuracy (data not shown).

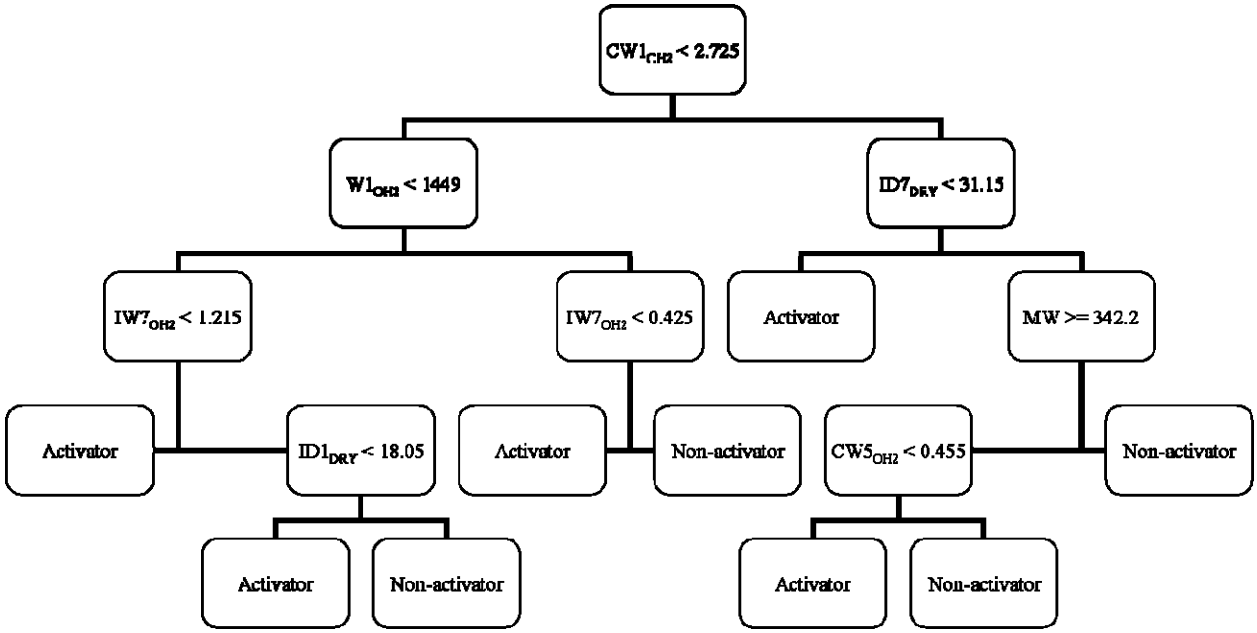

Figure 1. Recursive partitioning tree model separating PXR activators and PXR nonactivators developed in this study. The tree method is described in the Materials and Methods. Molecules are assigned to branches when descriptor values are greater than or less than a threshold value described in the preceding node. The subscripts represent the OH_2 and dry probe used in VolSurf calculations.

The RP method produces more interpretable models unlike those obtained from RF and SVM. The RP tree from the PXR activator and PXR nonactivator model is shown in Figure 1. In general, the descriptors important for PXR activators and PXR nonactivators are W1, CW1, CW5, IW7, ID1, ID7, and molecular weight (MW). These represent the first four descriptors from the OH_2 probe, and the next two are from the DRY probe. W1 accounts for polarizability and dispersion forces, CW1 and CW5 represent the extent of hydrophilic regions per surface unit, IW7 is an integer moment and measures the imbalance between the center of mass of a molecule and the hydrophilic regions around it, and ID1 and ID7 are also integer moments that measure the imbalance between the center of mass of a molecule and the hydrophobic regions around it. The RP tree can also be used to develop simple rules for separating PXR activators from PXR nonactivators.

When comparing predictions for individual molecules, we made the following observations: (i) Members of the initial test set of activators such as diflubenzuron are predicted as a nonactivator by all three machine learning methods in this study. Interestingly, the same molecule is also predicted as a PXR nonactivator by the PNN and *k*-NN models in a previous study that used the same training set (*20*). (ii) Fenbuconazole, another PXR activator from the previously used test set, is predicted as a PXR nonactivator by all of the models used previously (*20*), whereas the current RP and RF models correctly predicted it as a PXR activator in this study. The large test set used in this study contains 82 PXR activators and 63 nonactivators and is predominantly a subset of available drugs (*42*), imidazole derivatives similar to clotrimazole, steroids (*8*), molecules with different heterocyclic ring systems (*48*), and many other diverse molecules. In this large test set, the PXR nonactivators 5α-petromyzonol and 5*β*-cholan-3α,7α,12α,24-tetrol are predicted as PXR activators by all three QSAR methods in this study. The PXR activators 7-ketolithocholic acid and 12-ketolithocholic acid are predicted as PXR nonactivators by all three QSAR methods. Interestingly, the unsubstituted compound lithocholic acid is correctly predicted as a PXR activator by all three methods. The generally low affinity of PXR activators raises the possibility that for some of the molecules in the published data, toxicity of the compounds may complicate determination of PXR activation. It may also be possible to improve the predictions for PXR activation using additional different descriptors and modeling approaches.

Previously, we have used molecular similarity using the Tanimoto coefficient (*60*) or principal component analysis (PCA) to assess test and training set similarity (*61*). In our hands, either of these approaches is useful to understand potential outlier predictions. In this study, PCA was performed using VolSurf descriptors for the PXR data. The PCA score plot provides an estimate of the descriptor space of training and test set molecules (Figure 2) (*61*). Predictions can be considered as an extrapolation if the test set occupies a different descriptor space to the training set. It is clear from Figure 2 that the test set molecules occupy approximately the same descriptor space as that of the training set molecules, and one would therefore expect the predictions to be relatively accurate. The first three principal components of the training and test sets explain 55.6−68.6% of the variance, respectively. PCA analysis therefore did not explain the observed vs predicted PXR activation differences.

The logistic regression analysis method is a useful tool when the outcome of an experiment is binary (*62*), as in the current study either PXR activator or PXR nonactivator. Four different models were generated by docking molecules to the four available cocrystal structures for PXR. The FlexX scores were used as the independent variable, and the PXR activators or PXR nonactivators (class variables) were used as dependent variables in the logistic regression analysis. Two different confusion matrices were built for each crystal structure, that is, one using only successfully docked compounds and the other from both successfully docked and failed compounds. In the second case, molecules that failed to dock inside the LBD of PXR were considered as nonactivators. The logistic regression coefficients obtained from the FlexX scores were then used as the independent variable to predict activators/nonactivators in the test set. The best model was obtained using the structure with SR12813 (PDB ID: 1NRL), which resulted in eq 2 and

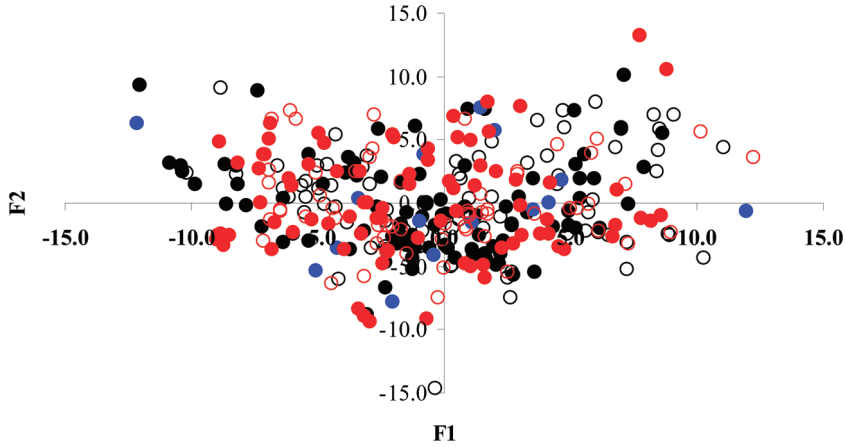

Figure 2. PCA scores plot of PXR training (*20*) and test and validation sets using the VolSurf descriptors. The PXR activators are shown as filled circles training (black), small test set ((*20*), blue), and large test set (red), whereas the nonactivators are shown as empty circles training (black) and large test set (red). This orthogonal linear transformation transforms the data to a new coordinate system. The *x*- and *y*-axes represent PCA scores from first and second principal components, respectively. The first three principal components of the training and test sets explain 55.6−68.6% of the variance, respectively.

was used to predict the large test set (Tables 1 and 2). The results for the other three complexes are not shown.

$$\text{Prob}(Y=\text{A}) = \frac{1}{1+e^{-(-0.0398\times\text{FlexX}-0.374)}} \quad \text{or}$$

$$\log \text{odds}(Y=\text{A}) = -0.374 - 0.0398\times\text{FlexX} \quad (2)$$

where Prob and A represent probability and activator, respectively. The value of the FlexX score is negative, and the associated coefficient is also negative (+0.0398), suggesting that the log odds (and, therefore, the probability) of a compound being a PXR activator decrease with the increase in FlexX score (positive value). In other words, for a one unit increase in FlexX score, the odds in favor of an activator are estimated to be decreased by a multiplicative factor of 0.961 (exp − 0.0398 = 0.961). Figure 3 shows several representative molecules from the test set that were correctly predicted as PXR activators by all methods in this study. Apart from the SE, which was higher for the test set than the machine learning methods, the performance of RF, SVM, and RP appears to be better than the docking logistic regression model, based on the prediction accuracies, SP, *Q*, and *C* of the large set (Table 1). The overall poor prediction accuracy of the docking results may be due to (i) poor performance of the scoring function in characterizing ligand−receptor interactions, (ii) treating the protein as rigid rather than flexible, and (iii) the overall promiscuous nature of the PXR LBD. It should also be noted that nine out of 145 (6.2%) test set molecules failed to dock and were classed as nonactivators, whereas predictions were made with the other machine learning models for all test set molecules.

Discussion

VolSurf descriptors have been widely used for drug discovery and ADME/Tox (*37–39, 63*). In the course of this study, we have developed novel predictive global models using VolSurf descriptors with human PXR activation classification data to identify compounds that are PXR activators. Such PXR activators may in turn lead to undesirable effects on drug and endogenous compound metabolism and transport. The machine learning models that we have evaluated in the course of this work can also be used for virtual screening to identify molecules previously unrecognized as PXR activators that can then be selected for in vitro testing. We have used a similar approach previously with transporters (*64, 65*). In this study, we have also used a large test set of 145 molecules that have not been included in model building to validate all of the computational approaches. Our classification results were a significant improvement on those published previously (*20*). It is important to note that the new test set was also structurally diverse yet covered the same descriptor space as the training set as analyzed using PCA analysis, which reassures us that we were unlikely to be extrapolating far beyond the training set (*61*). Although the results of the large test set are not as good as those achieved for internal validation of the training set, a common weakness of many computational approaches, this could be partially due to the promiscuous nature of PXR. We would add that in contrast to the previous study by Ung et al. (*20*) who used a test set of 15 PXR activators, we not only were able to predict more of these correctly, but we also further evaluated the model with a much larger test set and obtained predictions that we felt were acceptable considering the difficulty in predicting activation with this protein. The probabilities of randomly selecting a PXR activator or a PXR nonactivator are 56.55 and 43.44%, respectively. Our SVM results are therefore better than random for the large test set as we achieved approximately 68 and 65% correct for PXR activator or PXR nonactivator, respectively (Supplemental Table 2). These machine learning methods may be improved by using additional descriptor types, which we are currently evaluating for inclusion in future studies.

We have also utilized a structure-based docking approach using FlexX combined with logistic regression for comparison purposes, which performs poorly as compared with SVM, RP, and RF. This is perhaps not surprising considering the flexibility of PXR and the differences in the ligand-bound structures reported (*9, 10, 53, 54*). In this case, the final FlexX logistic regression model was based on 1NRL, which had a resolution of 2.00 Å (*9*). To our knowledge, there have been no direct comparisons of docking, QSAR, or machine learning methods for PXR with a large external test set containing diverse xenobiotics. Although a recent study has used both rigid and flexible docking to destabilize the key agonist−protein interactions for PXR in a small number of molecules, no binding scores or classification was reported (*35*). Assessment of other docking approaches in the future with a large test set like that used in the current analysis is justified in an attempt to improve the results and at least match the standard set by the machine learning models described herein. With several PXR crystal

Table 2. Prediction Results for the Large 145 Molecule Test Set[a]

compounds	classification	docking + logistic regression	RP	RF	SVM	reference/EC_{50} value determined in this study (μM)
1,9-dideoxydforskolin	A	N	A	A	A	*42*
amlodipine	A	A	A	A	N	*42*
bergamottin	A	N	A	A	A	*42*
celecoxib	A	A	A	N	N	*42*
diltiazem	A	A	A	N	A	*42*
felodipine	A	A	A	A	A	*42*
fluvastatin	A	A	N	A	A	*42*
forskolin	A	A	A	A	A	*42*
glimepiride	A	N (failed)	N	A	A	*42*
haloperidol	A	A	A	N	N	*42*
lansoprazole	A	A	A	N	N	*42*
mevastatin	A	N	A	A	A	*42*
montelukast	A	A	N	A	A	*42*
omeprazole	A	A	A	A	A	*42*
phenylbutazone	A	A	A	A	A	*42*
pioglitazone	A	A	A	A	A	*42*
rabeprazole	A	A	A	A	N	*42*
reserpine	A	N	A	N	N	*42*
rifabutin	A	N	A	A	A	*42*
rifapentine	A	N (failed)	A	N	N	*42*
CDD3508	A	A	A	A	A	*8*
CDD3532	A	A	A	A	A	*8*
CDD3538	A	A	A	A	A	*8*
CDD3543	A	A	A	A	A	*8*
CDD3501	A	A	A	A	A	*8*
CDD3530	A	A	A	A	A	*8*
CDD3536	A	A	A	A	A	*8*
CDD3540	A	A	A	A	A	*8*
5β-androstan-3α-ol	A	A	N	A	A	*8*
petromyzonol	N	N	A	A	A	*8*
17β-dihydroandrosterone	A	N	A	A	A	*8*
dihydrotestosterone	A	N	A	A	A	*8*
etiocholanolone	A	A	A	A	A	*8*
taurochenodeoxycholic acid	N	A	A	N	N	*8*
lithocholic acid	A	N	A	A	A	*8*
7-ketolithocholic acid	A	A	N	N	N	*8*
12-ketolithocholic acid	A	N	N	N	N	*8*
estrone	A	A	A	A	A	*8*
estriol	A	N	N	A	A	*8*
allocholic acid	N	N	A	N	N	*8*
cortolone	A	A	A	A	A	*8*
estetrol	A	N	N	A	A	*8*
epitestosterone sulfate	A	N	N	A	A	*8*
5β-pregnan-3α,20α-diol	A	N	A	A	A	*8*
5α-androstan-3α-ol	A	N	A	A	A	*8*
lithocholicacid acetate	A	N (failed)	A	A	A	*8*
5β-cholan-3α,7α,12α,24-tetrol	N	N	A	A	A	*8*
ω-muricholicacid	A	N	A	A	A	*8*
16,(5α)-androsten-3β-ol	A	N	A	A	A	*8*
tauro-β-muricholic acid	N	N	A	N	N	*8*
C2BA-10	A	A	A	N	N	*66*
C2BA-11	N	A	A	A	A	*66*
C2BA-12	N	A	A	A	A	*66*
C2BA-13	A	A	N	A	N	*66*
C2BA-248	A	A	N	A	N	*66*
C2BA-251	A	A	N	A	A	*66*
C2BA-3	N	A	A	A	N	*66*
C2BA-5	A	A	A	A	A	*66*
C2BA-6	A	A	A	N	A	*66*
C2BA-7	A	A	A	A	A	*66*
C2BA-8	A	A	A	A	A	*66*
C2BA-9	N	A	A	N	N	*66*
budesonide	A	A	A	A	A	*67*
carbamazepine	A	A	N	N	A	*68*
chlorpromazine	N	A	N	N	N	*69*
cyclophosphamide	A	N	A	A	A	*70*
efavirenz	A	A	N	N	N	*71*
etoposide	A	N	N	A	A	*71*
fluconazole	N	A	N	N	N	*72*
gemfibrozil	N	A	N	N	N	*73*
ketoconazole	N	N	N	A	A	*71*
nicardipine	A	A	A	N	N	*74*
rosiglitazone	A	A	A	N	A	*75*

Table 2. Continued

compounds	classification	docking + logistic regression	RP	RF	SVM	reference/EC_{50} value determined in this study (μM)
topotecan	A	N	N	N	A	*71*
valproic acid	A	N	N	A	A	*76*
bupropion	A	A	N	N	N	*42*
diclofenac	A	A	N	N	A	*42*
flutamide	A	A	N	N	N	*42*
isotretinoin	A	A	N	A	A	*42*
loratadine	A	A	A	N	N	*42*
meclizine	A	A	A	N	N	*42*
meloxicam	A	A	A	A	A	*42*
midazolam	A	A	A	N	N	*42*
nabumetone	A	A	A	A	A	*42*
naloxone	A	A	N	N	N	*42*
ondansetron	A	A	N	N	N	*42*
quinapril	A	A	A	N	N	*42*
raloxifene	A	A	A	N	A	*42*
sildenafil	A	A	N	N	N	*42*
simvastatin	A	N	A	A	A	*42*
terbinafine	A	A	N	N	N	*42*
triazolam	A	A	N	N	N	*42*
zolpidem	A	A	A	A	A	*42*
acetaminophen	N	A	A	A	A	*42* and inactive this study
acyclovir	N	A	N	N	N	*42*
albuterol	N	A	N	N	N	*42*
amitriptyline	N	A	N	N	N	*42*
atenolol	N	A	N	N	N	*42*
azithromycin	N	N (failed)	N	N	A	*42*
captopril	N	A	N	N	N	*42*
cimetidine	N	A	A	A	A	*42*
ciprofloxacin	N	A	A	N	N	*42*
clarithromycin	N	N (failed)	A	A	N	*42*
dapsone	N	A	A	A	N	*42*
desipramine	N	A	N	N	N	*42*
doxazosin	N	N	N	N	N	*42*
doxepin	N	A	N	N	N	*42*
doxorubicin	N	A	N	N	N	*42*
enalapril	N	N	A	A	A	*42*
erythromycin	N	N (failed)	A	A	A	*42*
ethosuximide	N	A	N	N	A	*42*
etodolac	N	A	N	N	A	*42*
famotidine	N	A	N	N	N	*42*
fexofenadine	N	N (failed)	A	N	N	*42*
furosemide	N	A	N	N	N	*42*
ibuprofen	N	A	N	A	A	*42*
lamotrigine	N	A	A	N	N	*42*
levofloxacin	N	A	N	N	N	*42*
linezolid	N	A	N	A	A	*42*
lisinopril	N	N (failed)	N	N	N	*42*
metoprolol	N	A	N	N	N	*42*
metronidazole	N	A	N	N	N	*42*
morphine	N	A	N	N	N	*42*
nadolol	N	A	N	N	A	*42*
naproxen	N	A	N	A	A	*42*
nevirapine	N	A	A	A	A	*42*
paroxetine	N	A	N	N	N	*42*
propranolol	N	A	N	N	N	*42*
ranitidine	N	N	N	N	N	*42*
risperidone	N	A	A	N	N	*42*
sumatriptan	N	A	N	N	N	*42*
tacrine	N	A	A	A	A	*42*
terazosin	N	A	A	A	A	*42*
theophylline	N	A	A	A	N	*42*
timolol	N	A	N	N	N	*42*
tocainide	N	A	N	N	N	*42*
tolmetin	N	A	N	N	N	*42*
valsartan	N	A	N	N	A	*42*
venlafaxine	N	N	N	N	N	*42*
zomitriptan	N	A	N	N	N	*42*
cholecalciferol	N	N (failed)	A	A	A	inactive, this study
flurbiprofen	A	A	N	N	N	80.1 μM, this study
mycophenolic acid	N	N	N	A	A	inactive, this study
oxcarbazepine	A	A	N	A	A	18.1 μM, this study
oxycodone	N	A	N	N	N	inactive, this study

[a] Classifications: A = PXR activator (agonist) and N = PXR nonactivator.

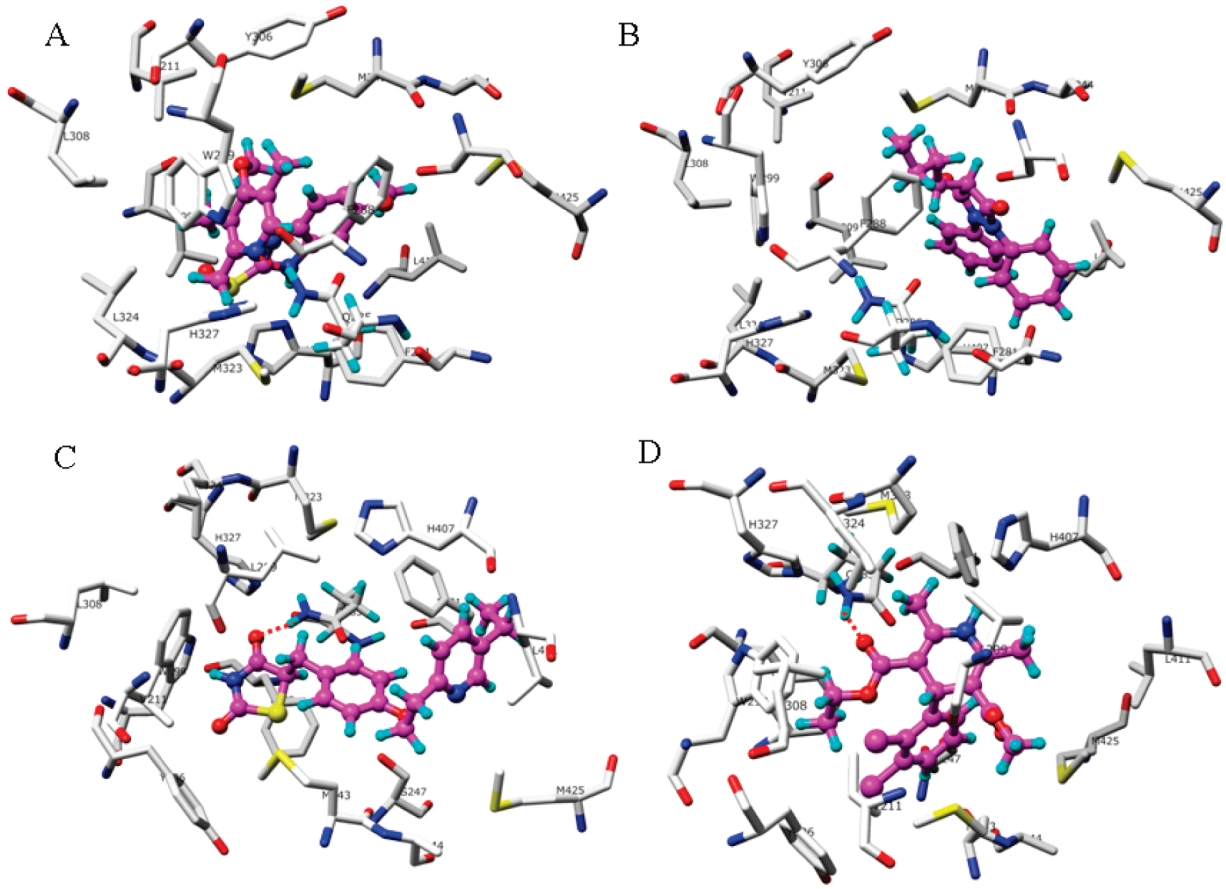

Figure 3. FlexX docked (1NRL) conformations of selected correctly predicted PXR activators—omeprazole (A), phenylbutazone (B), pioglitazone (C), and felodipine (D). Omeprazole, pioglitazone, and felodipine are predicted to form hydrogen-bonding interactions with the side chain NH of Gln-285. The hydrogen-bonding interaction is shown as red dotted lines. The amino acid residues are shown in the stick mode, whereas the PXR activators are shown in the ball and stick mode (purple). The 3D images were created using Chimera (*77*).

structures in the PDB (*9, 10, 53, 54*), this study has highlighted the difficulty in using docking to predict a large set of molecules as potential agonists and suggests that classification models developed with machine learning methods (*35*) may have an important role alongside pharmacophores (*8, 14*) and smaller "local" quantitative QSAR models in prioritizing compounds for in vitro testing. The combination of the training and test sets into a single larger model (322 molecules) would be worth assessing in the future with other descriptors and machine learning or docking methods and may lead to the creation of custom PXR scoring functions.

Although the docking approach was not ideal for classification, it could still be useful in those cases where the predictions were correct to enable a qualitative evaluation of the likely ligand−protein interactions. This could assist in defining what molecular changes can be introduced chemically to reduce or avoid PXR activation. For example, others have suggested attaching hydrogen-bonding groups on one of the hydrophobic features, adding larger more rigid groups, and removing central H-bond acceptors (*35*). The large test set created in this study (Table 2) can be used to find structurally similar compounds that are either observed human PXR activators or PXR nonactivators (regardless of their predicted activity) and provides further instruction as to what types of structural modification can decrease activity. While the test set contains numerous β-adrenergic blockers, they are all PXR nonactivators, and molecules in the calcium channel blocker and proton pump inhibitor series are all PXR activators. We were able to find some examples that had differing activity and visualize those that were correctly predicted as PXR activators based on the docking orientation. For example, oxycodone and morphine are PXR nonactivators, while naloxone is a PXR activator (Figure 4). While there are several subtle differences between the three compounds, naloxone contains an additional ethylene moiety, which may interact with a hydrophobic region in the LBD in addition to being a reactive functional group. Naproxen (PXR nonactivator) and nabumetone (PXR activator) are nonsteroidal anti-inflammatory drugs; the former possesses a carboxylic acid group, while the latter has a longer alkyl chain with a methyl substituted for the hydroxyl, which may serve to preferentially position the C═O hydrogen bond acceptor (Figure 4). Nevirapine is a PXR nonactivator, while oxcarbazepine and carbamazepine are PXR activators. The latter two molecules feature carboxamide moieties, which will serve as potential hydrogen bond acceptors, while in the corresponding position nevirapine has a hydrophobic group (Figure 4). A further series of tricyclic compounds includes the PXR nonactivators desipramine, doxepin, and amitriptyline, which contain a basic primary amine group at the end of an aliphatic chain, while the PXR activator loratadine has a neutral hydrogen bond acceptor in the corresponding position as well as ring substitutions. Interestingly, the training set also contains additional tricyclic molecules (protriptyline, nortriptyline, trimipramine, and clomipramine) that are PXR nonactivators; yet, structurally, they closely resemble desipramine, doxepin, and amitriptyline. These qualitative examples demonstrate some of the benefits of a large database of such binary classification information as it is valuable in biasing design of future molecules away from PXR activators that may be accomplished with the assistance of computational and in vitro methods.

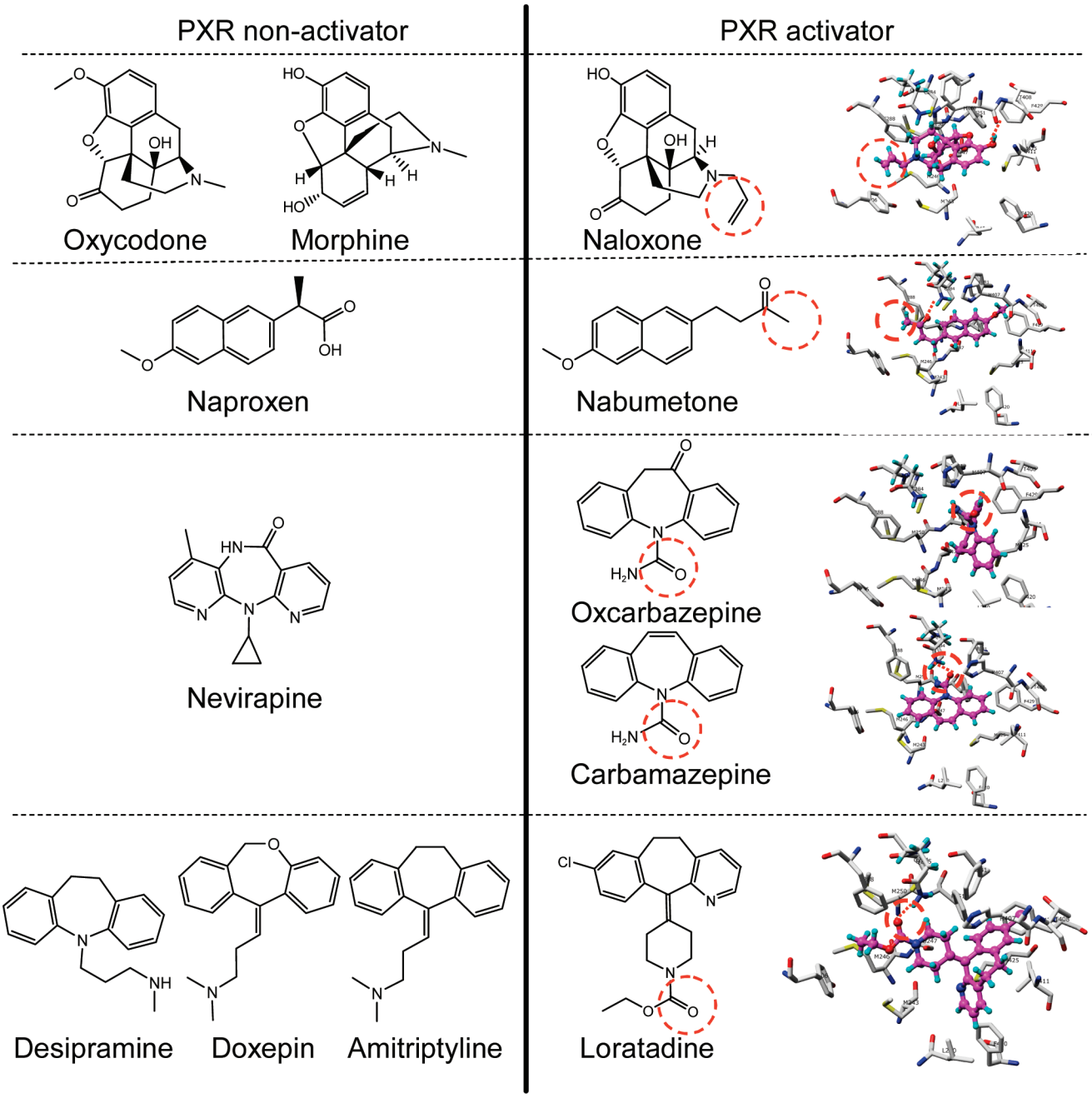

Figure 4. Examples of PXR nonactivator and PXR activator compounds in the test set that are structurally similar. Red dashed circles highlight likely important structural features that may contribute to activity. Corresponding PXR activator compounds (that had correctly predicted classifications) were docked in the PXR structure (1NRL) with FlexX (as described in the Materials and Methods). Carbamazepine (circled group), loratadine (circled group), and nabumetone (C═O group next to circled group) are predicted to form hydrogen-bonding interactions with the side chain NH of Gln-285; additionally, the methyl group in nabumetone may interact with the Phe288. Naloxone is predicted to form a H-bond with the side chain C═O and His407, and the ethylene group may also have a hydrophobic interaction with the Phe288. Oxcarbazepine docks differently to carbamazepine and may also form a H-bond between the side chain C═O and His407. The hydrogen-bonding interactions are shown as a red dotted line. The amino acid residues are shown in the stick mode, whereas the PXR activators are shown in the ball and stick mode (purple). The 3D images were created using Chimera (*77*).

In conclusion, we have developed new machine learning models (as well as docking models) for PXR that outperform those previously developed when tested with a new large external test set. We suggest that it is likely quite difficult to definitively describe functional groups that will globally decrease affinity due to the size and flexibility of the human PXR LBD; rather, as in this and previous cases (*35*), it will be important to address structural series individually using all of the available computational and in vitro tools at our disposal. These approaches should also enable increased efficiency of screening and testing, aiding pharmaceutical research to avoid developing potent PXR agonists.

Acknowledgment. M.D.K. is supported by K08-GM074238 from the National Institutes of Health and a Competitive Medical Research Fund (CMRF) grant from the University of Pittsburgh Medical Center. S.E. gratefully acknowledges Dr. Maggie A. Z. Hupcey for support and discussion and congratulates Dr. Kenneth Bachmann (University of Toledo) on his recent retirement.

Supporting Information Available: Molecules used in Table 2 in this study are available, along with the supplemental tables. This material is available free of charge via the Internet at http://pubs.acs.org.

References

(1) Bertilsson, G., Heidrich, J., Svensson, K., Asman, M., Jendeberg, L., Sydow-Backman, M., Ohlsson, R., Postlind, H., Blomquist, P., and Berkenstam, A. (1998) Identification of a human nuclear receptor defines a new signaling pathway for CYP3A induction. *Proc. Natl. Acad. Sci. U.S.A. 95*, 12208–12213.

(2) Blumberg, B., Sabbagh, W., Jr., Juguilon, H., Bolado, J., Jr., van Meter, C. M., Ong, E. S., and Evans, R. M. (1998) SXR, a novel steroid and xenobiotic-sensing nuclear receptor. *Genes Dev. 12*, 3195–3205.

(3) Kliewer, S. A., Moore, J. T., Wade, L., Staudinger, J. L., Watson, M. A., Jones, S. A., McKee, D. D., Oliver, B. B., Willson, T. M., Zetterstrom, R. H., Perlmann, T., and Lehmann, J. M. (1998) An orphan nuclear receptor activated by pregnanes defines a novel steroid signalling pathway. *Cell 92*, 73–82.

(4) Goodwin, B., Moore, L. B., Stoltz, C. M., McKee, D. D., and Kliewer, S. A. (2001) Regulation of the human CYP2B6 gene by the nuclear pregnane X receptor. *Mol. Pharmacol. 60*, 427–431.

(5) Staudinger, J. L., Goodwin, B., Jones, S. A., Hawkins-Brown, D., MacKenzie, K. I., LaTour, A., Liu, Y., Klaassen, C. D., Brown, K. K., Reinhard, J., Willson, T. M., Koller, B. H., and Kliewer, S. A. (2001) The nuclear receptor PXR is a lithocholic acid sensor that protects against liver toxicity. *Proc. Natl. Acad. Sci. U.S.A. 98*, 3369–3374.

(6) Synold, T. W., Dussault, I., and Forman, B. M. (2001) The orphan nuclear receptor SXR coordinately regulates drug metabolism and efflux. *Nat. Med. 7*, 584–590.

(7) Harmsen, S., Meijerman, I., Beijnen, J. H., and Schellens, J. H. (2007) The role of nuclear receptors in pharmacokinetic drug−drug interactions in oncology. *Cancer Treat. Rev. 33*, 369–380.

(8) Ekins, S., Chang, C., Mani, S., Krasowski, M. D., Reschly, E. J., Iyer, M., Kholodovych, V., Ai, N., Welsh, W. J., Sinz, M., Swaan, P. W., Patel, R., and Bachmann, K. (2007) Human pregnane X receptor antagonists and agonists define molecular requirements for different binding sites. *Mol. Pharmacol. 72*, 592–603.

(9) Watkins, R. E., Davis-Searles, P. R., Lambert, M. H., and Redinbo, M. R. (2003) Coactivator binding promotes the specific interaction between ligand and the pregnane X receptor. *J. Mol. Biol. 331*, 815–828.

(10) Watkins, R. E., Maglich, J. M., Moore, L. B., Wisely, G. B., Noble, S. M., Davis-Searles, P. R., Lambert, M. H., Kliewer, S. A., and Redinbo, M. R. (2003) 2.1A crystal structure of human PXR in complex with the St John's Wort compound hyperforin. *Biochemistry 42*, 1430–1438.

(11) Watkins, R. E., Noble, S. M., and Redinbo, M. R. (2002) Structural insights into the promiscuity and function of the human pregnane X receptor. *Curr. Opin. Drug Discovery Dev. 5*, 150–158.

(12) Watkins, R. E., Wisely, G. B., Moore, L. B., Collins, J. L., Lambert, M. H., Williams, S. P., Willson, T. M., Kliewer, S. A., and Redinbo, M. R. (2001) The human nuclear xenobiotic receptor PXR: Structural determinants of directed promiscuity. *Science 292*, 2329–2333.

(13) Xue, Y., Moore, L. B., Orans, J., Peng, L., Bencharit, S., Kliewer, S. A., and Redinbo, M. R. (2007) Crystal structure of the pregnane X receptor-estradiol complex provides insights into endobiotic recognition. *Mol. Endocrinol. 21*, 1028–1038.

(14) Ekins, S., and Erickson, J. A. (2002) A pharmacophore for human pregnane-X-receptor ligands. *Drug Metab. Dispos. 30*, 96–99.

(15) Bachmann, K., Patel, H., Batayneh, Z., Slama, J., White, D., Posey, J., Ekins, S., Gold, D., and Sambucetti, L. (2004) PXR and the regulation of apoA1 and HDL-cholesterol in rodents. *Pharmacol. Res. 50*, 237–246.

(16) Schuster, D., Laggner, C., Steindl, T. M., Palusczak, A., Hartmann, R. W., and Langer, T. (2006) Pharmacophore modeling and in silico screening for new P450 19 (aromatase) inhibitors. *J. Chem. Inf. Model. 46*, 1301–1311.

(17) Ekins, S., Mirny, L., and Schuetz, E. G. (2002) A ligand-based approach to understanding selectivity of nuclear hormone receptors PXR, CAR, FXR, LXRa and LXRb. *Pharm. Res. 19*, 1788–1800.

(18) Jacobs, M. N. (2004) In silico tools to aid risk assessment of endocrine disrupting chemicals. *Toxicology 205*, 43–53.

(19) Ekins, S., Andreyev, S., Ryabov, A., Kirillov, E., Rakhmatulin, E. A., Sorokina, S., Bugrim, A., and Nikolskaya, T. (2006) A combined approach to drug metabolism and toxicity assessment. *Drug Metab. Dispos. 34*, 495–503.

(20) Ung, C. Y., Li, H., Yap, C. W., and Chen, Y. Z. (2007) In silico prediction of pregnane X receptor activators by machine learning approaches. *Mol. Pharmacol. 71*, 158–168.

(21) Wang, C. Y., Li, C. W., Chen, J. D., and Welsh, W. J. (2006) Structural model reveals key interactions in the assembly of the pregnane X receptor/corepressor complex. *Mol. Pharmacol. 69*, 1513–1517.

(22) Tetko, I. V., Bruneau, P., Mewes, H. W., Rohrer, D. C., and Poda, G. I. (2006) Can we estimate the accuracy of ADME-Tox predictions? *Drug Discovery Today 11*, 700–707.

(23) Dimitrov, S., Dimitrova, G., Pavlov, T., Dimitrova, N., Patlewicz, G., Niemela, J., and Mekenyan, O. (2005) A stepwise approach for defining the applicability domain of SAR and QSAR models. *J. Chem. Inf. Model. 45*, 839–849.

(24) Sheridan, R. P., Feuston, B. P., Maiorov, V. N., and Kearsley, S. K. (2004) Similarity to molecules in the training set is a good discriminator for prediction accuracy in QSAR. *J. Chem. Inf. Comput. Sci. 44*, 1912–1928.

(25) Muegge, I., and Enyedy, I. J. (2004) Virtual screening for kinase targets. *Curr. Med. Chem. 11*, 693–707.

(26) Kubinyi, H. (2006) Success stories of computer-aided design. In *Computer Applications in Pharmaceutical Research and Development* (Ekins, S., Ed.) pp 377−424, John Wiley and Sons, Hoboken, NJ.

(27) Ekins, S., Mestres, J., and Testa, B. (2007) In silico pharmacology for drug discovery: Applications to targets and beyond. *Br. J. Pharmacol. 152*, 21–37.

(28) Ekins, S., Mestres, J., and Testa, B. (2007) In silico pharmacology for drug discovery: Methods for virtual ligand screening and profiling. *Br. J. Pharmacol. 152*, 9–20.

(29) Costache, A. D., Trawick, D., Bohl, D., and Sem, D. S. (2007) AmineDB: large scale docking of amines with CYP2D6 and scoring for druglike properties-towards defining the scope of the chemical defense against foreign amines in humans. *Xenobiotica 37*, 221–245.

(30) Kitchen, D. B., Decornez, H., Furr, J. R., and Bajorath, J. (2004) Docking and scoring in virtual screening for drug discovery: methods and applications. *Nat. Rev. Drug Discovery 3*, 935–949.

(31) Ghosh, S., Nie, A., An, J., and Huang, Z. (2006) Structure-based virtual screening of chemical libraries for drug discovery. *Curr. Opin. Chem. Biol. 10*, 194–202.

(32) Leach, A. R., Shoichet, B. K., and Peishoff, C. E. (2006) Prediction of protein-ligand interactions. Docking and scoring: Successes and gaps. *J. Med. Chem. 49*, 5851–5855.

(33) Cummings, M. D., DesJarlais, R. L., Gibbs, A. C., Mohan, V., and Jaeger, E. P. (2005) Comparison of automated docking programs as virtual screening tools. *J. Med. Chem. 48*, 962–976.

(34) Charifson, P. S., Corkery, J. J., Murcko, M. A., and Walters, W. P. (1999) Consensus scoring: A method for obtaining improved hit rates from docking databases of three-dimensional structures into proteins. *J. Med. Chem. 42*, 5100–5109.

(35) Gao, Y. D., Olson, S. H., Balkovec, J. M., Zhu, Y., Royo, I., Yabut, J., Evers, R., Tan, E. Y., Tang, W., Hartley, D. P., and Mosley, R. T. (2007) Attenuating pregnane X receptor (PXR) activation: A molecular modelling approach. *Xenobiotica 37*, 124–138.

(36) Jones, G., Willett, P., Glen, R. C., Leach, A. R., and Taylor, R. (1997) Development and validation of a genetic algorithm for flexible docking. *J. Mol. Biol. 267*, 727–748.

(37) Doddareddy, M. R., Cho, Y. S., Koh, H. Y., Kim, D. H., and Pae, A. N. (2006) In silico renal clearance model using classical Volsurf approach. *J. Chem. Inf. Model. 46*, 1312–1320.

(38) Cruciani, G., Crivori, P., Carrupt, P. A., and Testa, B. (2000) Molecular fields in quantitative structure-permeation relationships: The VolSurf approach. *THEOCHEM* 17–30.

(39) Ooms, F., Weber, P., Carrupt, P. A., and Testa, B. (2002) A simple model to predict blood-brain barrier permeation from 3D molecular fields. *Biochim. Biophys. Acta 1587*, 118–125.

(40) Kramer, B., Rarey, M., and Lengauer, T. (1999) Evaluation of the FLEXX incremental construction algorithm for protein-ligand docking. *Proteins 37*, 228–241.

(41) Zhang, T., Zhou, J. H., Shi, L. W., Zhu, R. X., and Chen, M. B. (2007) 3D-QSAR studies with the aid of molecular docking for a series of non-steroidal FXR agonists. *Bioorg. Med. Chem. Lett. 17*, 2156–2160.

(42) Sinz, M., Kim, S., Zhu, Z., Chen, T., Anthony, M., Dickinson, K., and Rodrigues, A. D. (2006) Evaluation of 170 xenobiotics as transactivators of human pregnane X receptor (hPXR) and correlation to known CYP3A4 drug interactions. *Curr. Drug Metab. 7*, 375–388.

(43) Faucette, S. R., Zhang, T. C., Moore, R., Sueyoshi, T., Omiecinski, C. J., LeCluyse, E. L., Negishi, M., and Wang, H. (2007) Relative activation of human pregnane X receptor versus constitutive androstane receptor defines distinct classes of CYP2B6 and CYP3A4 inducers. *J. Pharmacol. Exp. Ther. 320*, 72–80.

(44) Zhu, Z., Kim, S., Chen, T., Lin, J. H., Bell, A., Bryson, J., Dubaquie, Y., Yan, N., Yanchunas, J., Xie, D., Stoffel, R., Sinz, M., and Dickinson, K. (2004) Correlation of high-throughput pregnane X receptor (PXR) transactivation and binding assays. *J. Biomol. Screening 9*, 533–540.

(45) Krasowski, M. D., Yasuda, K., Hagey, L. R., and Schuetz, E. G. (2005) Evolution of the pregnane x receptor: Adaptation to cross-species differences in biliary bile salts. *Mol. Endocrinol. 19*, 1720–1739.

(46) Krasowski, M. D., Yasuda, K., Hagey, L. R., and Schuetz, E. G. (2005) Evolutionary selection across the nuclear hormone receptor superfamily with a focus on the NR1I subfamily (vitamin D, pregnane X, and constitutive androstane receptors). *Nucl. Recept. 3*, 2.

(47) Weininger, D. (1988) SMILES 1. Introduction and encoding rules. *J. Chem. Inf. Comput. Sci. 28*, 31.
(48) Lemaire, G., Benod, C., Nahoum, V., Pillon, A., Boussioux, A. M., Guichou, J. F., Subra, G., Pascussi, J. M., Bourguet, W., Chavanieux, A., and Balaguer, P. (2007) Discovery of a highly active ligand of human Pregnane X Receptor: a case study from pharmacophore modeling and virtual screening to "in vivo" biological activity. *Mol. Pharmacol. 72*, 572–581.
(49) Clark, M. A., Cramer, R. D., and van Op den Bosch, N. (1989) Validation of the general purpose Tripos 5.2 force field. *J. Comput. Chem. 10*, 982–1012.
(50) Therneau, T. M. and Atkinson, E. J. (1997) An Introduction to Recursive Partitioning Using the RPART Routines. Department of Health Sciences Research, Mayo Clinic.
(51) Liaw, A., and Wiener, M. (2002) Classification and regression by random forest. *R News 2/3*, 18–22.
(52) Hsu, C.-W., Chang, C.-C., and Lin, C.-J. (2008) A practical guide to support vector classification; http://www.csie.ntu.edu.tw/~cjlin/papers/guide/guide.pdf.
(53) Chrencik, J. E., Orans, J., Moore, L. B., Xue, Y., Peng, L., Collins, J. L., Wisely, G. B., Lambert, M. H., Kliewer, S. A., and Redinbo, M. R. (2005) Structural disorder in the complex of human pregnane X receptor and the macrolide antibiotic rifampicin. *Mol. Endocrinol. 19*, 1125–1134.
(54) Xue, Y., Chao, E., Zuercher, W. J., Willson, T. M., Collins, J. L., and Redinbo, M. R. (2007) Crystal structure of the PXR-T1317 complex provides a scaffold to examine the potential for receptor antagonism. *Bioorg. Med. Chem. 15*, 2156–2166.
(55) Krovat, E. M., and Langer, T. (2004) Impact of scoring functions on enrichment in docking-based virtual screening: An application study on renin inhibitors. *J. Chem. Inf. Comput. Sci. 44*, 1123–1129.
(56) Oloff, S., Mailman, R. B., and Tropsha, A. (2005) Application of validated QSAR models of D1 dopaminergic antagonists for database mining. *J. Med. Chem. 48*, 7322–7332.
(57) Zhang, Q., and Muegge, I. (2006) Scaffold hopping through virtual screening using 2D and 3D similarity descriptors: Ranking, voting, and consensus scoring. *J. Med. Chem. 49*, 1536–1548.
(58) Ekins, S., Durst, G. L., Stratford, R. E., Thorner, D. A., Lewis, R., Loncharich, R. J., and Wikel, J. H. (2001) Three dimensional quantitative structure permeability relationship analysis for a series of inhibitors of rhinovirus replication. *J. Chem. Inf. Comput. Sci. 41*, 1578–1586.
(59) So, S.-S., and Karplus, M. (1999) A comparitive study of ligand-receptor complex binding affinity prediction methods based on glycogen phosphorylase inhibitors. *J. Comput.-Aided Mol. Des. 13*, 243–258.
(60) Ekins, S., Balakin, K. V., Savchuk, N., and Ivanenkov, Y. (2006) Insights for human ether-a-go-go-related gene potassium channel inhibition using recursive partitioning, Kohonen and Sammon mapping techniques. *J. Med. Chem. 49*, 5059–5071.
(61) Khandelwal, A., Bahadduri, P., Chang, C., Polli, J. E., Swaan, P., and Ekins, S. (2007) Computational models to assign biopharmaceutics drug disposition classification from molecular structure. *Pharm. Res. 24*, 2249–2262.
(62) Jones, D. R., Ekins, S., Li, L., and Hall, S. D. (2007) Computational approaches that predict metabolic intermediate complex formation with CYP3A4 (+b5). *Drug Metab. Dispos. 35*, 1466–1475.
(63) Berellini, G., Cruciani, G., and Mannhold, R. (2005) Pharmacophore, drug metabolism, and pharmacokinetics models on non-peptide AT1, AT2, and AT1/AT2 angiotensin II receptor antagonists. *J. Med. Chem. 48*, 4389–4399.
(64) Chang, C., Ekins, S., Bahadduri, P., and Swaan, P. W. (2006) Pharmacophore-based discovery of ligands for drug transporters. *Adv. Drug Delivery Rev. 58*, 1431–1450.
(65) Ekins, S., Johnston, J. S., Bahadduri, P., D'Souzza, V. M., Ray, A., Chang, C., and Swaan, P. W. (2005) In vitro and pharmacophore based discovery of novel hPEPT1 inhibitors. *Pharm. Res. 22*, 512–517.
(66) Lemaire, G., Benod, C., Nahoum, V., Pillon, A., Boussioux, A. M., Guichou, J. F., Subra, G., Pascussi, J. M., Bourguet, W., Chavanieux, A., and Balaguer, P. (2007) Discovery of a highly active ligand of human Pregnane X receptor: A case study from pharmacophore modeling and virtual screening to "in vivo" biological activity. *Mol. Pharmacol. 72*, 572–581.
(67) Maier, A., Zimmermann, C., Beglinger, C., Drewe, J., and Gutmann, H. (2007) Effects of budesonide on P-glycoprotein expression in intestinal cell lines. *Br. J. Pharmacol. 150*, 361–368.
(68) Luo, G., Cunningham, M., Kim, S., Burn, T., Lin, J., Sinz, M., Hamilton, G. A., Rizzo, C., Jolley, S., Gilbert, D., Downey, A., Mudra, D., Graham, R., Carroll, K., Xie, J., Madan, A., Parkinson, A., Christ, D., Selling, B., LeCluyse, E. L., and Gan, L.-S. (2002) CYP3A4 induction by drugs: Correlation between a pregnane X receptor reporter gene assay and CYP3A4 expression in human hepatocytes. *Drug Metab. Dispos. 30*, 795–804.
(69) Hartley, D. P., Dai, X., Yabut, J., Chu, X., Cheng, O., Zhang, T., He, Y. D., Roberts, C., Ulrich, R., Evers, R., and Evans, D. C. (2006) Identification of potential pharmacological and toxicological targets differentiating structural analogs by a combination of transcriptional profiling and promoter analysis in LS-180 and Caco-2 adenocarcinoma cell lines. *Pharmacogenet. Genomics 16*, 579–599.
(70) Lindley, C., Hamilton, G., McCune, J. S., Faucette, S., Shord, S. S., Hawke, R. L., Wang, H., Gilbert, D., Jolley, S., Yan, B., and LeCluyse, E. L. (2002) The effect of cyclophosphamide with and without dexamethasone on cytochrome P450 3A4 and 2B6 in human hepatocytes. *Drug Metab. Dispos. 30*, 814–822.
(71) Chang, T. K., and Waxman, D. J. (2006) Synthetic drugs and natural products as modulators of constitutive androstane receptor (CAR) and pregnane X receptor (PXR). *Drug Metab. Rev. 38*, 51–73.
(72) Duret, C., Daujat-Chavanieu, M., Pascussi, J. M., Pichard-Garcia, L., Balaguer, P., Fabre, J. M., Vilarem, M. J., Maurel, P., and Gerbal-Chaloin, S. (2006) Ketoconazole and miconazole are antagonists of the human glucocorticoid receptor: consequences on the expression and function of the constitutive androstane receptor and the pregnane X receptor. *Mol. Pharmacol. 70*, 329–339.
(73) Prueksaritanont, T., Richards, K. M., Qiu, Y., Strong-Basalyga, K., Miller, A., Li, C., Eisenhandler, R., and Carlini, E. J. (2005) Comparative effects of fibrates on drug metabolizing enzymes in human hepatocytes. *Pharm. Res. 22*, 71–78.
(74) Drocourt, L., Pascussi, J. M., Assenat, E., Fabre, J. M., Maurel, P., and Vilarem, M. J. (2001) Calcium channel modulators of the dihydropyridine family are human pregnane X receptor activators and inducers of CYP3A, CYP2B, and CYP2C in human hepatocytes. *Drug Metab. Dispos. 29*, 1325–1331.
(75) Ogino, M., Nagata, K., and Yamazoe, Y. (2002) Selective suppressions of human CYP3A forms, CYP3A5 and CYP3A7, by troglitazone in HepG2 cells. *Drug Metab. Pharmacokinet. 17*, 42–46.
(76) Cerveny, L., Svecova, L., Anzenbacherova, E., Vrzal, R., Staud, F., Dvorak, Z., Ulrichova, J., Anzenbacher, P., and Pavek, P. (2007) Valproic acid induces CYP3A4 and MDR1 gene expression by activation of constitutive androstane receptor and pregnane X receptor pathways. *Drug Metab. Dispos. 35*, 1032–1041.
(77) Pettersen, E. F., Goddard, T. D., Huang, C. C., Couch, G. S., Greenblatt, D. M., Meng, E. C., and Ferrin, T. E. (2004) UCSF Chimera-a visualization system for exploratory research and analysis. *J. Comput. Chem. 25*, 1605–1612.

TX800102E